

Semiconducting single-walled carbon nanotubes exposed to distilled water and aqueous solution: Electrical measurement and theoretical calculation

Ming-Pei Lu, Cheng-Yun Hsiao, Po-Yuan Lo, Jeng-Hua Wei, Yuh-Shyong Yang, and Ming-Jer Chen

Citation: *Applied Physics Letters* **88**, 053114 (2006); doi: 10.1063/1.2172014

View online: <http://dx.doi.org/10.1063/1.2172014>

View Table of Contents: <http://scitation.aip.org/content/aip/journal/apl/88/5?ver=pdfcov>

Published by the [AIP Publishing](#)

Articles you may be interested in

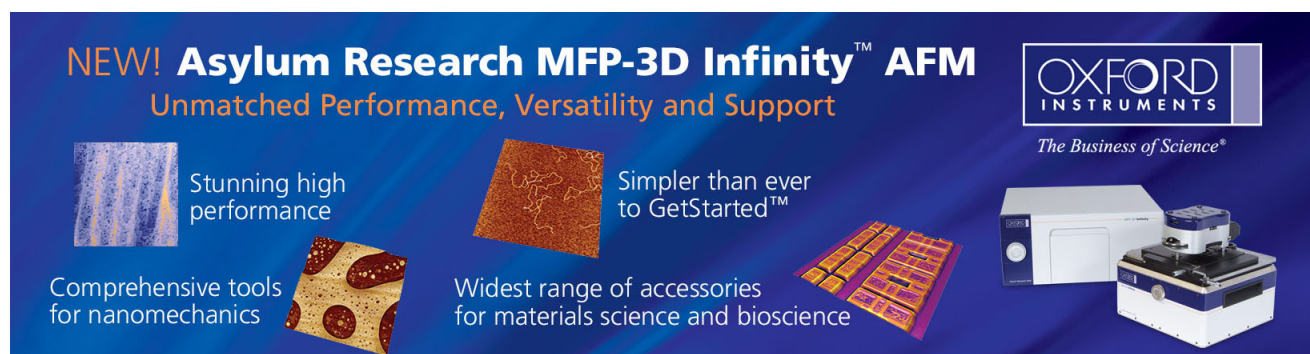
[Terahertz detection mechanism and contact capacitance of individual metallic single-walled carbon nanotubes](#)
Appl. Phys. Lett. **100**, 163503 (2012); 10.1063/1.4704152

[Photosensitivity of solution-based indium gallium zinc oxide single-walled carbon nanotubes blend thin film transistors](#)
Appl. Phys. Lett. **94**, 102112 (2009); 10.1063/1.3098406

[Gate capacitance in electrochemical transistor of single-walled carbon nanotube](#)
Appl. Phys. Lett. **88**, 073104 (2006); 10.1063/1.2173626

[Pronounced hysteresis and high charge storage stability of single-walled carbon nanotube-based field-effect transistors](#)
Appl. Phys. Lett. **87**, 133117 (2005); 10.1063/1.2067690

[Conductance measurement of single-walled carbon nanotubes in aqueous environment](#)
Appl. Phys. Lett. **82**, 2338 (2003); 10.1063/1.1566084

The advertisement features a dark blue background with white and orange text. At the top left, it reads 'NEW! Asylum Research MFP-3D Infinity™ AFM' in large white letters, followed by 'Unmatched Performance, Versatility and Support' in orange. To the right is the Oxford Instruments logo, which includes the text 'OXFORD INSTRUMENTS' and the tagline 'The Business of Science®'. Below the text are four images: a textured surface, a grid of small circular patterns, a grid of small rectangular patterns, and the physical AFM instrument. Text descriptions are placed around these images: 'Stunning high performance' next to the textured surface, 'Simpler than ever to GetStarted™' next to the grid of small circular patterns, 'Comprehensive tools for nanomechanics' next to the grid of small rectangular patterns, and 'Widest range of accessories for materials science and bioscience' next to the AFM instrument.

Semiconducting single-walled carbon nanotubes exposed to distilled water and aqueous solution: Electrical measurement and theoretical calculation

Ming-Pei Lu

Department of Electronics Engineering, National Chiao Tung University, Hsin-Chu, Taiwan

Cheng-Yun Hsiao

Department of Biological Science and Technology, National Chiao Tung University, Hsin-Chu, Taiwan

Po-Yuan Lo and Jeng-Hua Wei

Electronics Research & Service Organization, Industrial Technology Research Institute (ERSO/ITRI), Hsin-Chu, Taiwan

Yuh-Shyong Yang^{a)}

Department of Biological Science and Technology, National Chiao Tung University, Hsin-Chu, Taiwan

Ming-Jer Chen^{b)}

Department of Electronics Engineering, National Chiao Tung University, Hsin-Chu, Taiwan

(Received 2 May 2005; accepted 19 December 2005; published online 1 February 2006)

We fabricate and measure a single-walled carbon nanotube transistor having a liquid-gate electrode. The ratio value of $I_{\text{on}}/I_{\text{off}}$ is as high as 10^4 , indicating the presence of a semiconducting channel. A passivation layer over the source/drain electrode greatly suppresses the liquid-gate leakage by about three orders of magnitude. The channel currents are noticeably distinct between two liquid samples: distilled water and aqueous solution (1×10^{-4} M NaCl). This biological sensing ability is attributed to the different electrical double-layer capacitances with respect to the bulk part of the channel. The corresponding theoretical calculation is carried out in detail. © 2006 American Institute of Physics. [DOI: 10.1063/1.2172014]

Since Iijima¹ discovered the basic carbon nanotube (CNT) structure in 1991, there have been today a large number of research teams worldwide to examine the potentials of the carbon nanotube. It is well recognized that the single-walled carbon nanotubes can be seen as a quasi-one-dimensional conductor^{2,3} and can behave in a metallic or semiconducting way depending upon its diameter and chirality.^{4,5} The first CNT field-effect transistor (FET) with the experimental input-output transfer characteristics was reported in 1998.^{6,7} Since CNT is highly sensitive to a nearby charge, the device can further find such applications as gas sensor.^{8,9} The CNT also can exhibit sensitivities to the electrolyte solution via a liquid gate.¹⁰ However, there were few articles in the literature to address electrical properties of the CNTs that are directly exposed to different liquid samples such as the distilled water and aqueous solution. Here we present one such study on a single-walled carbon nanotube FET having a liquid gate, which is fabricated using conventional processes, followed by the theoretical calculation.

A 300 nm thick Si_3N_4 layer was grown on the silicon wafer, followed by a 100 nm thick titanium (Ti) metal that was sputtered and subsequently patterned as the source/drain electrode. The spacing between the source and drain electrode was $2 \mu\text{m}$. The single-walled carbon nanotubes¹¹ were immersed in dimethylformamide (DMF) undergoing the ultrasound wave and spread across the substrate. Then an 800 nm thick photoresist (PR) was laid on the wafer and through patterning, a wide slit¹² was created. The photoresist

remaining on the source/drain electrode can serve as a passivation layer. By controlling in advance the density of the immersed CNTs, we achieved a single CNT or a CNT bundle bridging the gap as depicted in Fig. 1. A liquid-gate electrode¹³ was set up to develop an electrochemical potential in the electrolyte with respect to the CNT surface. A micropipette was employed to place a small ($\sim 1\text{--}0.5 \mu\text{l}$) electrolyte droplet into the open slit. The measurement setup is schematically shown in Fig. 1.

The measured drain current for CNTs exposed to both the distilled water (resistivity $\sim 18.2 \text{ M}\Omega \text{ cm}$) and aqueous solution (1×10^{-4} M NaCl) for a certain device is plotted in

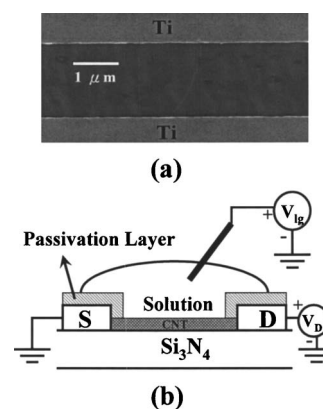


FIG. 1. (a) The SEM image of the top side of a device with a CNT bundle bridging the gap, which was formed before the photoresist process; and (b) the measurement setup. The source electrode is grounded, the drain electrode is tied to V_D and the liquid-gate electrode is connected to V_{lg} . The passivation layer keeps the source and drain electrode from the solution.

^{a)}Electronic mail: ysyang@faculty.nctu.edu.tw

^{b)}Electronic mail: chenmj@faculty.nctu.edu.tw

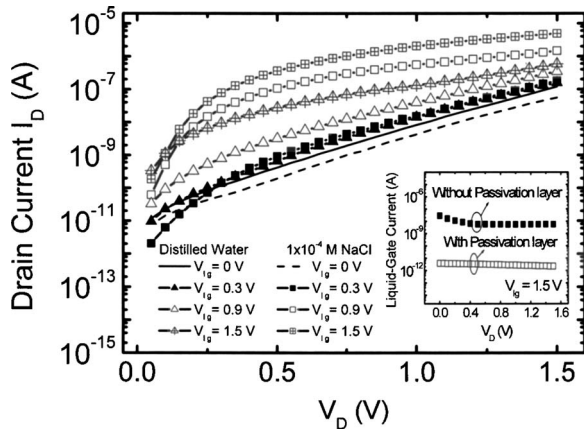


FIG. 2. The measured drain current versus drain voltage for both the distilled water and aqueous solution with the liquid-gate voltage as a parameter. The inset shows the liquid-gate current in the distilled water case with and without a passivation layer at $V_{lg}=1.5$ V.

Fig. 2 versus drain voltage with the liquid-gate voltage V_{lg} as a parameter (0, 0.3, 0.9, and 1.5 V). Evidently, a change in the liquid material can produce a noticeable change in drain current, especially at high V_{lg} . We also obtained similar results for the other device samples. Therefore, the biological sensing ability is confirmed. Indeed, the ratio value of I_{on}/I_{off} in Fig. 2 is as high as 10^4 , indicating the presence of a semi-conducting channel rather than a metallic one. This is consistent with the fact that the intrinsic conductance associated with a metallic CNT is a weak function of the liquid-gate voltage.¹⁴ The above measurement was performed in the presence of a passivation layer over the drain/source electrode. The corresponding liquid-gate current falls below around 10^{-12} A in a wide range of drain voltage. For the case of no passivation layer (that is, no photoresist utilized), we obtained the liquid-gate current of order of 10^{-9} A as shown in the inset of Fig. 2 for the distilled water case. Hence, the presence of a passivation layer can substantially reduce the liquid-gate leakage current by about three orders of magnitude. In addition, since the passivation layer can prevent oxygen molecules from adsorbing on the surface of the drain/source electrode, a relatively low Schottky barrier in favor of electron injection can be expected, meaning the n -type operation.¹⁵

Although the drain current level is very low due to conventional manufacturing processes adopted (i.e., Ti metal), the drain current significantly changes as the liquid solution changes as depicted in Fig. 2. Such remarkable change can be attributed to the different electrical double-layer capacitances with respect to the quantum capacitance of the bulk part of the CNTs, rather than the contact counterpart. This argument is consistent with the use of a passivation layer that can prohibit the contact from the water molecule adsorption. The corresponding theoretical calculation is demonstrated below.

To facilitate the analysis, the work is concentrated on the high drain voltage regime over which the effect of the drain-side Schottky barrier can be ignored. The measured conductance of the CNTs at high drain voltages is plotted in Fig. 3(a) versus V_{lg} , showing that the threshold gate voltage for CNTs exposed to distilled water is around 0.77 V while for the 1×10^{-4} M NaCl solution it is about 0.32 V. When the liquid-gate voltage reaches the threshold value, the conduc-

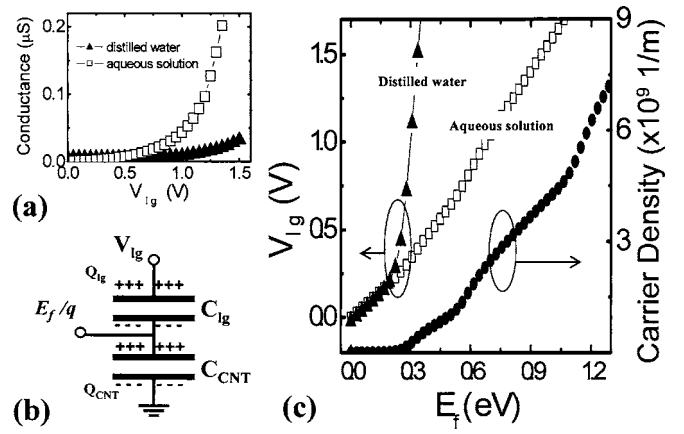


FIG. 3. (a) The measured conductance for CNTs exposed to the distilled water (\blacktriangle) and aqueous solution (\square) in the high drain voltage region; (b) the capacitive equivalent circuit seen from the liquid-gate electrode to the underlying CNTs; and (c) the calculated V_{lg} vs Fermi level for CNTs exposed to the distilled water (\blacktriangle) and aqueous solution (\square), as well as the carrier density vs Fermi level.

tion band coincides with the Fermi level in the bulk part of CNTs. Above the threshold point, the charge starts to accumulate in the CNTs and turns on the device. To describe different threshold voltages between different liquid samples, a capacitance model in a liquid-gate electrode to underlying bulk channel system, as depicted in Fig. 3(b), is utilized. Here C_{lg} is the electrical double-layer capacitance between CNTs and ions, and C_{CNT} is the quantum capacitance for CNTs. A relevant relation for the undoped carbon nanotubes can readily be established from this equivalent circuit,¹³

$$qV_{lg} = E_f + q \cdot \frac{Q_{CNT}}{C_{lg}}, \quad (1)$$

where Q_{CNT} is the charge density per unit length and E_f is the Fermi level relative to the middle bandgap energy. The carrier density of CNTs can be written as

$$Q_{CNT} = \sum_i q \int_{E_i}^{\infty} D_i(E) \cdot f(E) dE, \quad (2)$$

where E_i is the bottom of the i th conduction subband relative to the middle band gap energy; $f(E)$ is the Fermi-Dirac distribution; and $D_i(E)$ is the density of states given by¹⁶

$$D_i = \frac{8}{3\pi \cdot a \cdot |V_{pp\pi}|} \frac{|E|}{\sqrt{E^2 - E_i^2}} \quad \text{for } E \geq E_i, \quad (3)$$

where E is the electron energy relative to the middle band gap energy; $a \approx 0.144$ nm corresponds to the carbon-carbon bond distance; and $V_{pp\pi} \approx 2.5$ eV represents the nearest-neighbor overlap interaction energy.

As for double-layer capacitance in (1), it is usually treated as an ideal cylindrical capacitance by $C_{lg} = 2\pi\epsilon\epsilon_0/\ln(1+2\lambda_D/d)$, where ϵ ($\epsilon_{H_2O} \approx 80$) is the dielectric constant, d is the carbon nanotube diameter, and λ_D is the Debye screening length. For 1×10^{-4} M NaCl solution, taking $d=1.4$ nm (for $E_g \approx 0.56$ eV) (Ref. 2) and typically $\lambda_D = 31$ nm, one obtains $C_{lg} = 1.162$ nF/m. For distilled water, the Debye screening length is about $1 \mu\text{m}$, comparable to the distance from the liquid-gate electrode to CNTs, meaning that the center of the equipotential surface around the double-layer capacitance is unlikely to be located at the cen-

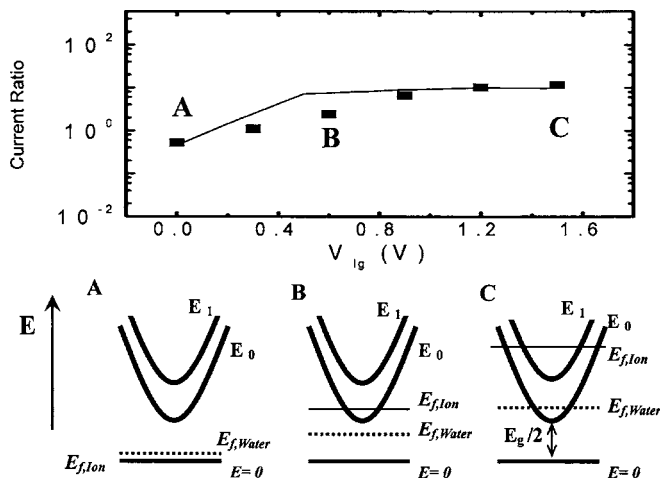


FIG. 4. The ratio (■) of measured drain current in aqueous solution to that in distilled water vs liquid-gate voltage. The solid line is the corresponding calculated Q_{CNT} ratio. Also displayed are the positions of the Fermi level relative to the common one-dimensional subband diagram, respectively, corresponding to three operating points.

ter of the CNT cross section. The ideal cylindrical capacitance may not be suitable for the case of the CNTs exposed to the distilled water. Thus we suggest $C_{lg} \approx 55$ pF/m for distilled water, rather than use of the ideal double-layer capacitance (~ 613 pF/m). The double-layer capacitance of aqueous solution or distilled water is much larger than quantum capacitance at low liquid-gate voltages, indicating that the quantum capacitance prevails in the liquid-gate to CNTs system ($V_{lg} \approx E_f/q$). On the other hand, at high liquid-gate voltages, the double-layer capacitance of aqueous solution is comparable to the quantum capacitance in determining the relation between liquid-gate voltage and Fermi level, whereas the double-layer capacitance of distilled water is less than the quantum capacitance. Therefore, the double-layer capacitance dominates in the distilled water capacitance system operated at high liquid-gate voltages. Since C_{lg} is known, the V_{lg} can be calculated against E_f using (1) as plotted in Fig. 3(c). Also depicted in Fig. 3(c) is the carrier density per unit length from (2). Evidently, the threshold voltage for distilled water and aqueous solution is 0.75 and 0.28 V, respectively, quite close to the experimental values in Fig. 3(b). In addition, we found that the ratio of Q_{CNT} in aqueous solution to that in distilled water is quantitatively close to the corresponding measured drain current ratio, as displayed in Fig. 4 against V_{lg} . It can also be seen that the current ratio initially increases with V_{lg} and then tends to saturate. This is consistent with the Q_{CNT} ratio, corroborating the validity of the calculation work. Also together plotted in Fig. 4 is the corresponding positioning of the Fermi level: (a) at $V_{lg} = 0$ V labeled A, the Fermi level ($E_{f,Water}$) for CNT exposed to distilled water is higher than Fermi level ($E_{f,Ion}$) for CNTs exposed to aqueous solution; (b) as V_{lg} increases to the point B ($V_{lg} = 0.6$ V), the $E_{f,Ion}$ is increased faster than $E_{f,Water}$; and (c) at higher liquid-gate voltage C ($V_{lg} = 1.5$ V), the $E_{f,Ion}$ crosses the second lowest subband (E_1) while the $E_{f,Water}$ just exceeds the first lowest subband (E_0).

Note that in Fig. 2 for $V_{lg} = 0$, the drain current for distilled water is almost two times that for aqueous solution. The plausible origin may be that the H_2O molecule is stably adsorbed on the CNTs surface (despite low probability at room temperature), causing CNTs operation from p to n -type.¹⁷ This means that some charge is transferred from a single H_2O to CNTs. We further assume that the distilled water has higher H_2O molecule density than aqueous solution; so H_2O molecules are likely to be adsorbed on the CNTs, especially for the case of distilled water. We then take a doping level with 0.02 eV for distilled water while keeping undoped Fermi level for aqueous solution. The H_2O molecules transfer about $5000e^-$ per unit length; that is, each H_2O molecule can transfer about $0.03e^-$.¹⁸ If we take the average distance between H_2O molecules of about 0.3 nm, the probability for the H_2O molecule adsorption is found to be very low ($\sim 10^{-6}$). Thus, the effect of the doping is simply to shift the V_{lg} by 0.02 V for a fixed E_f .¹³

We perform electrical measurement of the CNTs exposed to the distilled water and aqueous solution. The biological sensing ability of the fabricated devices and its physical origin have been confirmed. Theoretical calculation is carried out in detail, which can adequately elucidate experimental data and can provide insights such as the positioning of the Fermi level.

The authors are grateful to the Industrial Technology Research Institute (ERSO/ITRI) for the fabrication of the test devices, and to Min-Chieh Chuang, Yu-Ming Chang, and Bai-Hong Cheng for experimental assistance. This work was supported by the National Science Council under Contract No. NSC 93-2215-E-009-002.

¹S. Iijima, Nature (London) **354**, 56 (1991).

²J. W. G. Wildöer, L. C. Venema, A. G. Rinzler, R. E. Smalley, and C. Dekker, Nature (London) **391**, 59 (1998).

³T. W. Odom, J.-L. Huang, P. Kim, and C. M. Lieber, Nature (London) **391**, 62 (1998).

⁴J. W. Mintmire, B. I. Dunlap, and C. T. White, Phys. Rev. Lett. **68**, 631 (1992).

⁵R. Saito, M. Fujita, G. Dresselhaus, and M. S. Dresselhaus, Appl. Phys. Lett. **60**, 2204 (1992).

⁶S. J. Tans, A. R. M. Verschueren, and C. Dekker, Nature (London) **393**, 49 (1998).

⁷R. Martel, T. Schmidt, H. R. Shea, T. Hertel, and Ph. Avouris, Appl. Phys. Lett. **73**, 2447 (1998).

⁸J. Kong, N. R. Franklin, C. Zhou, M. G. Chapline, S. Peng, K. Cho, and H. Dai, Science **287**, 622 (2000).

⁹P. G. Collins, K. Bradley, M. Ishigami, and A. Zettl, Science **287**, 1801 (2000).

¹⁰S. Rosenblatt, Y. Yaish, J. Park, J. Gore, V. Sazonova, and P. L. McEuen, Nano Lett. **2**, 869 (2002).

¹¹The single-walled carbon nanotubes with a diameter of 1.4 nm were supplied by Carbon Nanotechnologies Incorporated (CNI).

¹²T. Someya, P. Kim, and C. Nuckolls, Appl. Phys. Lett. **82**, 2338 (2003).

¹³M. Krüger, M. R. Buitelaar, T. Nussbaumer, C. Schönenberger, and L. Forró, Appl. Phys. Lett. **78**, 1291 (2001).

¹⁴P. G. Collins, M. S. Arnold, and Ph. Avouris, Science **292**, 706 (2001).

¹⁵V. Derycke, R. Martel, J. Appenzeller, and Ph. Avouris, Appl. Phys. Lett. **80**, 2773 (2002).

¹⁶J. W. Mintmire and C. T. White, Phys. Rev. Lett. **81**, 2506 (1998).

¹⁷A. Zahab, L. Spina, P. Poncharal, and C. Marlière, Phys. Rev. B **62**, 10000 (2000).

¹⁸R. Pati, Y. Zhang, S. K. Nayak, and P. M. Ajayan, Appl. Phys. Lett. **81**, 2638 (2002).